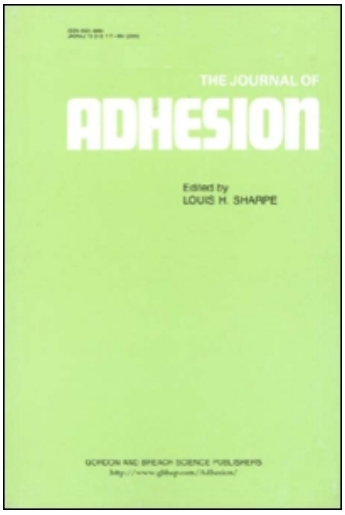

The Journal of Adhesion
Publication details, including instructions for authors and subscription information:
http://www.informaworld.com/smpp/title~content=t713453635

ION-ION CORRELATIONS IN LIQUID DISPERSIONS

Bo Jönsson[a]; Håkan Wennerström[a]
[a] Theoretical Chemistry and Physical Chemistry l, Chemical Center, Lund University, Lund, Sweden

Online publication date: 10 August 2010

To cite this Article Jönsson, Bo and Wennerström, Håkan(2004) 'ION-ION CORRELATIONS IN LIQUID DISPERSIONS', The Journal of Adhesion, 80: 5, 339 — 364
To link to this Article: DOI: 10.1080/00218460490465551
URL: http://dx.doi.org/10.1080/00218460490465551

The Journal of Adhesion, 80: 339–364, 2004

ISSN: 0021-8464 print/1545-5823 online
DOI: 10.1080/00218460490465551

Taylor & Francis
Taylor & Francis Group

ION–ION CORRELATIONS IN LIQUID DISPERSIONS

Bo Jönsson
Håkan Wennerström
Theoretical Chemistry and Physical Chemistry l, Chemical Center, Lund University, Lund, Sweden

Ion–ion correlations play an important role in liquid dispersion with strong electrostatic interactions. Examples can be found in very diverse areas with the setting of cement paste as one extreme and the compactation of DNA as another. One particularly spectacular effect of ion–ion correlations is that the traditional double layer repulsion sometimes can be converted into a net attraction. This typically takes place in the presence of multivalent counterions and/or in solutions with low dielectric permittivity. The attractive forces are driven by the energy while the repulsive are mainly of entropic origin, and the final outcome is a delicate balance of these contributions. Here we present two simple models, which give a conceptually simple description of this balance.

Keywords: Electric double layer; Ion-ion correlation; Attractive forces; Monte Carlo simulation; Multivalent ions; Surfactant systems

INTRODUCTION

Colloidal particles, biopolymers, and membranes all carry charges in an aqueous environment. The molecular source of these charges can be covalently bound ionic groups like phosphates, sulfates, carboxylates, quartenary ammoniums, or protonated amines. The carboxylates and amines can titrate in response to *pH* changes, while other groups remain charged except at extreme conditions. A particle, a self-assembled aggregate, or a polymer can also acquire a charge by

Received 7 October 2003; in final form 10 March 2003.

One of a collection of papers honoring Jacob Israelachvili, the recipient in February 2003 of *The Adhesion Society Award for Excellence in Adhesion Science, Sponsored by 3M*.

Address correspondence to Bo Jönsson, Theoretical Chemistry and Physical Chemistry l, Chemical Center, Lund University, POB 124, SE-22100 Lund, Sweden. E-mail: bo.jonsson@teokem.lu.se

adsorption of a small charged molecule. The interactions between charged mesoscopic objects is strongly influenced by the net charge, and the electrostatic interactions provide one of the basic organizing principles in both colloidal sols and in living cells. These interactions can be both attractive, leading to association, and repulsive, resulting in dispersion.

The basic description of electrostatic interactions between colloidal particles was worked out during the 1940s independently by Derjaguin and Landau in the Soviet Union [1] and by Verwey and Overbeek in the Netherlands [2]. Both groups based their description of the electrostatic effects on the Poisson-Boltzmann (PB) equation. Combined with a description of van der Waals interactions, the resulting DLVO theory has played an immense role in our understanding and description of interactions in liquid dispersions.

As all theories, the DLVO approach has its limitations coming from both the model and approximations. The theory is based on a continuum description of two media separated by a sharp interface. All real interfaces have a finite width, and the DLVO theory can be expected to work properly only at separations that exceed this width. Another more intriguing source of a breakdown of the DLVO description is the mean field approximation inherent in the PB equation. This article is focused on this effect, and we start with a conceptual discussion of ion–ion correlations and continue with a development of two simple model systems amenable to trivial numerical solutions. Next the effects of the geometrical shape of the colloidal entities are treated. We conclude by giving a number of examples of experimental manifestations of correlation effects.

GENERAL ASPECTS ON CHARGE–CHARGE CORRELATIONS

Charge-charge correlation is a general mechanism for generating attractive interactions in molecular and atomic systems. The textbook example is the dispersion interaction operating between any two atoms or molecules. In a conventional description it is caused by correlations between electrons in the two interacting atoms (molecules), and it invokes a quantum mechanical description of the degrees of freedom.

There exist, however, other well-known examples of attractive interactions due to charge–charge correlations involving *classical* degrees of freedom, *e.g.,* the Debye interaction between a permanent dipole and a polarizability and the Keesom interaction between two rotating dipoles at a finite temperature [3]. These can be expressed in terms of polarizabilities, α, of the two species k and l, giving

$$V_{ij}(R) = -\frac{3k_BT\alpha_k\alpha_l}{(4\pi\varepsilon_0)^2R^\theta}, \tag{1}$$

where R is the separation. In fact, the quantum mechanical dispersion interaction goes asymptotically to this form, demonstrating the fundamental connection between these interactions due to charge–charge correlations [4]. Ion–ion correlations can also give an interaction of precisely this form if the ions are confined in space [5]. Consider two spherical cells, each of radius R_c and each containing one spherical macroion of charge z_M and radius R_M plus neutralizing counterions (see Figure 1). A distance R separates the macroion centers.

The excess free energy, ΔA, due to the interaction of the two subsystems is according to statistical mechanical perturbation theory,

$$\Delta A = -k_BT\ln\langle\exp[-\Delta V(R)/k_BT]\rangle_0 \approx -\frac{\langle\Delta V(R)^2\rangle_0}{2k_BT}, \tag{2}$$

where $\Delta V\ (R)$ is the interaction energy between the cells for a particular configuration of counterions. The angular brackets, $\langle\ \rangle_0$, represent an average over the counterions in the individual noninteracting cells. The interaction energy, $\Delta V(R)$, can be written as a two-center multipole expansion, where the different terms represent charge–charge, charge–dipole, and dipole–dipole interactions, etc. For electroneutral subsystems the lowest order term contributing to ΔA is due to the dipole–dipole component,

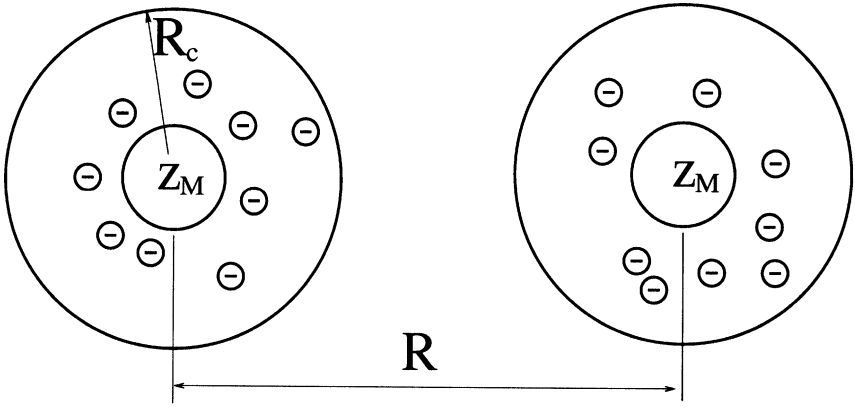

FIGURE 1 Two interacting but nonoverlapping charge distributions, each with a central macromolecule of charge z_Me surrounded by neutralizing counterions.

$$\Delta V(R) \approx \sum_i \sum_j \frac{z_i z_j e^2}{4\pi\varepsilon_0\varepsilon_r R^3}(r_i r_j - 3r_{ix} r_{jx}), \tag{3}$$

where the summation over i and j are for the two subsystems, respectively. Using the spherical symmetry of the subsystems,

$$\langle \Delta V(R)^2 \rangle_0 \approx 6\Big(\frac{1}{4\pi\varepsilon_0\varepsilon_r R^3}\Big)^2 \Big\langle \Big(\sum_i z_i e r_{ix}\Big)^2 \Big\rangle_0 \Big\langle \Big(\sum_j z_j e r_{jx}\Big)^2 \Big\rangle_0, \tag{4}$$

where the polarizability, α, can be identified as

$$\alpha = \frac{\langle (\sum_i z e r_{ix})^2 \rangle_0}{k_B T}. \tag{5}$$

If combining Equations (2–5), then the free energy of interaction can be written as

$$\Delta A = -\frac{3k_B T \alpha_k \alpha_i}{(4\pi\epsilon_0\epsilon_r)^2 R^\theta}, \tag{6}$$

illustrating the generality of Equation (1) and the analogy with the dispersion force. The only difference between Equations (1) and (6) is in the dielectric permittivity, ϵ_r, of the medium.

Another example of ion–ion correlations in spherical geometry is the case with two droplets formed from an aqueous electrolyte solution, which will interact according to Equation (6) and the polarizabilities will be those of conducting spheres. A similar case is obtained with reversed micelles (or water in oil microemulsion droplets) formed by ionic surfactants [6].

Even for net neutral (dipolar) surfaces there is always a lateral charge distribution and correlations with another similar surface will lead to attraction [7]. The in-plane and the out-of-plane dipolar components behave qualitatively differently, since the former can correlate by change of orientation, while the latter requires a translational motion to achieve the attractive effect. The magnitude of these interactions depends on the interactions within the surface, while the distance dependence is generic [8–11]. A particularly interesting case occurs when one has a structure on a mesoscopic scale in the surface due to surface aggregates or domains. Due to the large size of the correlating entities one can easily reach a direct interaction that clearly exceeds $k_B T$, meaning that the system is strongly correlated. The interaction is then more long ranged, except asymptotically, and can lead to a strong attraction exceeding that predicted by the Lifshitz theory even at large separations [12–14].

ION–ION CORRELATIONS IN PARALLEL LINEAR SYSTEMS

Some polyelectrolytes, such as the DNA double helix and viruses, as well as self-assembled surfactant aggregates can occur as charges stiff rods. In an aqueous medium the interaction between these highly charged rods is dominated by electrostatics. In order to obtain a complete description of the system one has to analyze the interaction between rods of arbitrary orientation [15], but the simpler case of parallel rods is particularly relevant when considering correlation effects. A pioneering study of this case was made by Oosawa [16], who used as ion condensation model with separate populations of (1) diffuse ions and (2) ions condensed on the polyelectrolyte backbone. The latter could be seen as a one-dimensional conductor. Using a perturbation method Oosawa arrived at an expression for the attractive force component (per unit length) due to "charge fluctuations,"

$$f(R) \simeq -k_B T \frac{(z\zeta)^2}{1+(z\zeta)^2} \frac{1}{R^2} + \cdots, \tag{7}$$

where R is the rod–rod separation, $l_B = e^2/4\pi\epsilon_0\epsilon_r k_B T$ is the Bjerrum length, and $\zeta = l_B/b$ with b equal to the length per unit charge on the polyelectrolyte backbone. For a system like DNA with b = 1.7 Å and $l_B = 7.1$ Å at ambient conditions, this force is only weakly dependent on counterion valency and it *increases* linearly with temperature.

Forces due to charge fluctuations in the long wavelength limit are typically included in the general Lifshitz theory of van der Waals forces [3]. A straightforward implementation of this point of view would predict a distance dependence of the force of R^{-6} rather than R^{-2}. This discrepancy reveals an interesting difference between the linear system on one hand and the planar and spherical systems on the other. In the latter cases the coefficients for the "classical" [17] contribution remain finite as the dielectric permittivity of the bodies diverges, while for parallel cylinders it diverges. Oosawa's derivation demonstrates that in the conducting limit the interaction changes from R^{-6} to R^{-2}. Oosawa's result is based on a perturbation expansion focused on the asymptotic behaviour for large separations where long wavelength "charge fluctuations" give rise to the attractive forces. At closer separation the main contribution to the force comes from short wavelength fluctuations. For charges on a line the lowest energy is obtained by ordering the counterions with a separation zb, and for not too-high temperatures the structure factor peaks at $2\pi m/zb$, where m is a small integer number. Grønbech-Jensen *et al.* [18] arrived at an approximate free energy of interaction due to correlations of this type of charge distribution;

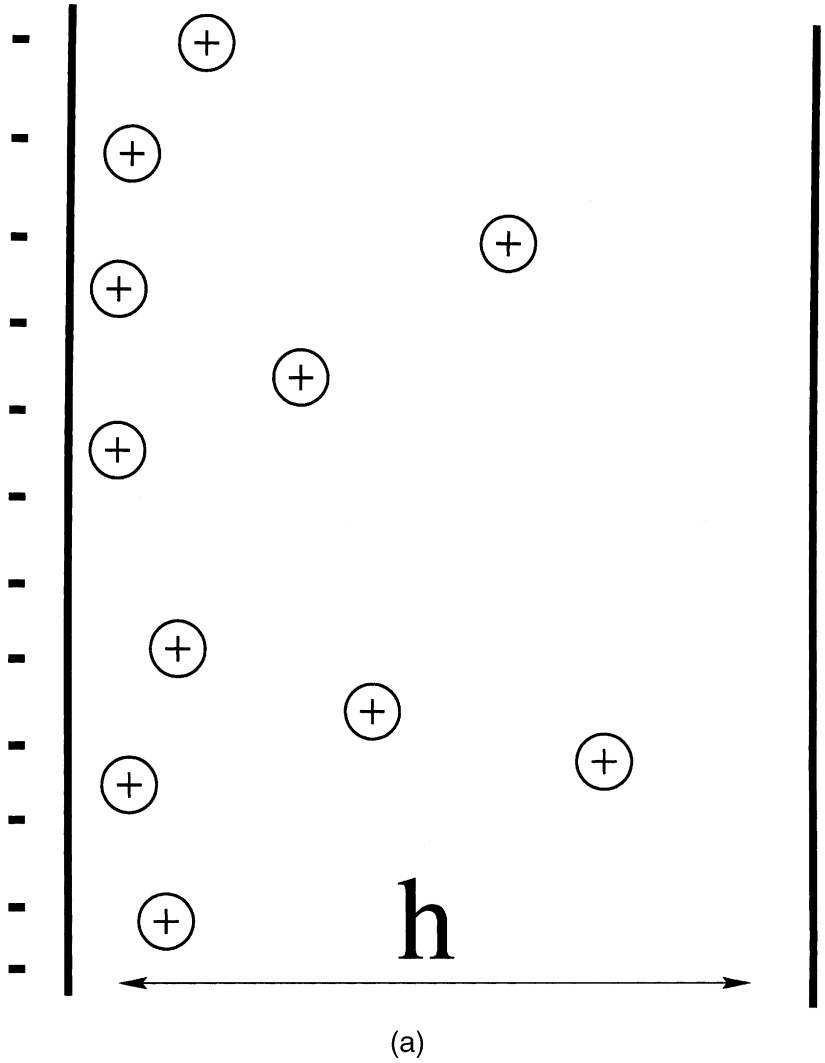

FIGURE 2 (a) Schematic representation of a single charged wall and its counterions. (b) Same as in (a), but with two charged surfaces. Additional salt pairs have been left out for clarity. (*Continued*).

$$V(R) = -\frac{k_B T}{zb}(z\zeta)^3 \ln(z\zeta) K_0^2(2\pi k/zb) \tag{8}$$

where K_0 is a modified Bessel function. Since $\zeta \propto T^{-1}$, this contribution increases in importance at low temperature in contrast to the

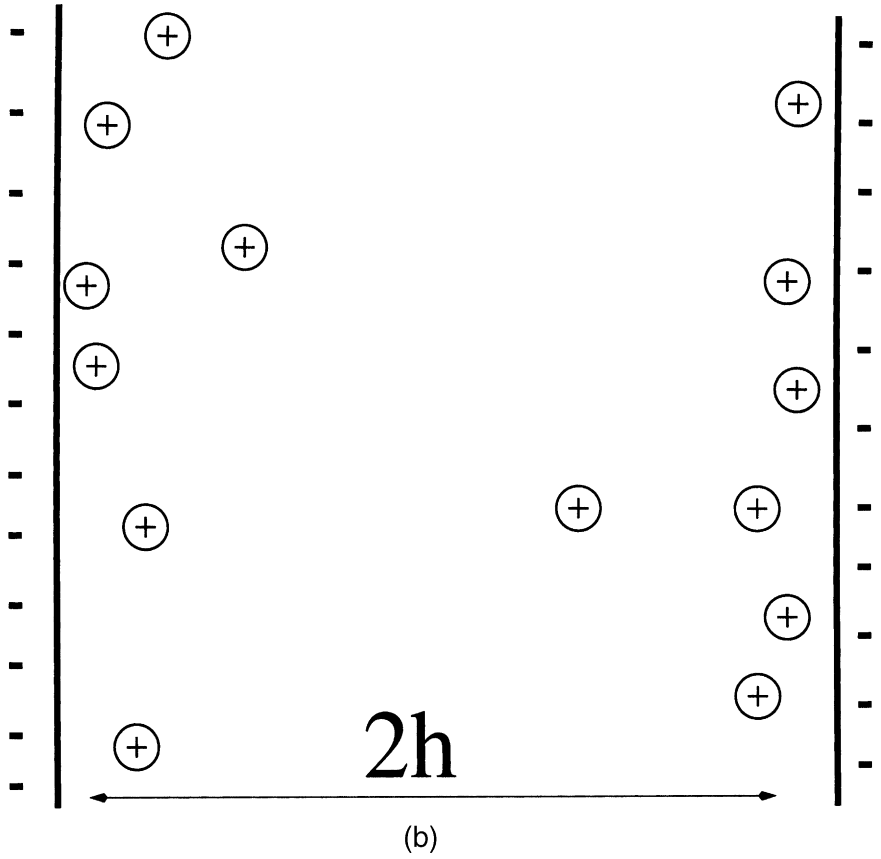

FIGURE 2 (Continued).

Oosawa result, *cf* Equation (7). The "charge fluctuation" contribution considered by Oosawa, with its opposite temperature dependence, is part of the asymptotic van der Waals contribution and is numerically less relevant for short and intermediate separations. In Equation (8) the attraction also increases strongly with counterion valency. It is this type of correlation that gives rise to the strong deviations from DLVO theory, which are the focus of the present article and were first demonstrated by Guldbrand *et al.* for two charged planes [9] as well as two cylinders [20].

In the models used by Oosawa and Grønbech-Jensen *et al.* the attractive and repulsive electrostatic components are treated as being due to separate counterion populations. In a real system there is no

clear basis for such a dichotomy, and both components are affected by ion–ion correlations. This interplay between the direct correlation attraction and double layer repulsion is more clearly analyzed in a planar geometry.

ION–ION CORRELATIONS IN PLANAR SYSTEMS

One way to derive the (PB) equation is by replacing the ion–ion pair correlation function with a product of one particle densities [21]. To get an illustration of the implications of such an approximation let us compare two situations in a planar geometry. In the first case we have one charged wall with surface charge density σ and one neutral surface separated by distance h. Between the walls we have counterions and possibly some electrolyte. The pressure in this system is given by the ion concentration at the neutral surface. In the second case we have two charged surfaces separated by $2h$ (see Figure 2). Physically the situations are clearly different. If we apply the standard boundary conditions of the PB equation, one finds that ion distributions in the first case are identical to the ion distribution of the two halves in the second case and that the forces between the walls are identical. In an exact treatment of the model this will not be true, since there are interactions between ions on either half of the midplane. We can write an exact expression for the osmotic pressure [22]:

$$p_{\sigma\delta m} = k_B T \sum_i [c_i(\text{mid-plane}) + p_i^{corr} + p_i^{hc}]. \tag{9}$$

The term p_i^{corr} comes from the fact that the ions on either side of the mid-plane correlate and it will give an attractive contribution to the pressure. In the mean field description there is no interaction across the midplane due to electroneutrality. A further difference from the PB description is that in the exact treatment the size of the ions plays a role, *i.e.*, we get the hard core term p_i^{hc}, which in principle could be included in the correlation term, but it is sometimes informative to calculate the two terms, *i.e.*, the pressure due to electrostatic and hard-core correlations, separately. In some cases the neglect of correlations and ion size will compensate each other and the numerical validity of the PB results is extended [23].

In order to study the role of ion–ion correlations from a conceptual point of view it is a virtue to go to an as simple as possible model where such effects can appear. The case of two parallel planar, similarly charged walls separated by a medium containing only counterions represents the most simple yet realistic case. In

the PB description the solution is characterized by a single dimensionless parameter [24]:

$$K_1 = \frac{-\sigma zeh}{2k_B T \epsilon_0 \epsilon_r} = \frac{h}{\lambda_{GC}}, \tag{10}$$

where we have introduced the Gouy-Chapman length, $\lambda_{GC} = e/2\pi z\sigma l_B$. In an exact treatment only one additional dimensionless parameter is required, provided one lets the counterion radius go to zero [19]:

$$K_2 = \frac{z^4 l_B^2}{h\lambda_{GC}}. \tag{11}$$

As long as the ion radius is small enough, *i.e.*, the Bjerrum length is much larger than the ion radius, the effect of the counterion radius is small in the counterion-only case, since close ion–ion encounters are excluded by the electrostatic repulsion. Excluding electrolyte ions sometimes appears unphysical, but there are in fact a number of systems where the counterion concentration is much larger than the concentration of neutral salt. Lyotropic liquid crystals formed by ionic amphiphiles and cement paste are two examples where this condition is met [25, 26].

We should expect ion–ion correlations to be important when the average Coulomb interaction between the ions is substantial relative to $k_B T$. Equation (11) tells us that the ion valency is the most important factor; it also happens to be easily varied experimentally.

It turns out that for aqueous systems at ambient temperatures the ion–ion correlation effects become important for systems with di- or multivalent counterions. This was demonstrated by Monte Carlo (MC) simulations by Guldbrand *et al.* [19] and confirmed by solutions of the inhomogeneous hypernetted chain equation (HNC) by kjellander and Marčelja [27, 28] and by additional MC simulations by Valleau *et al.* [29] and also by Bratko and Vlachy [30]. The modified PB equation, due to Outhwaite and Bhuiyan [31, 32], has also provided further insight into the approximations in the PB equation [33]. In Figure 3 we show results of ion–ion correlation effects for different valency of the counterions. With monovalent counterions the pressure is repulsive over the whole range of physically accessible surface charge densities even if substantial corrections can occur, in particular with highly charged surfaces at close separations [34]. Divalent and even more trivalent counterions lead to strong attractive forces already at modest surface charge densities. In the two latter cases the entropic term in Equation (9) rapidly goes to zero, and the interaction is dominated by the correlation term.

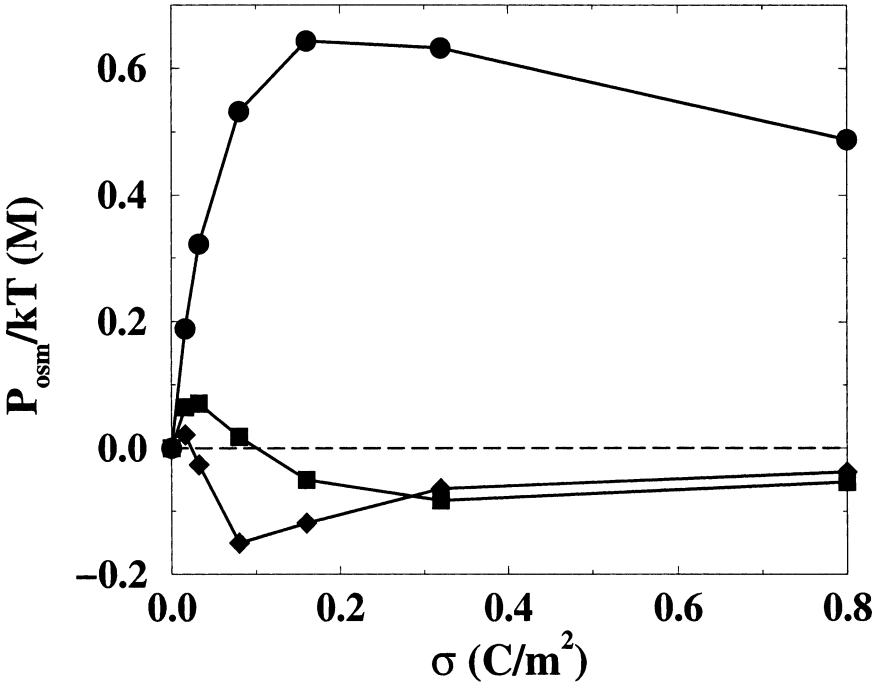

FIGURE 3 The osmotic pressure as a function of surface charge density for two planar double layers with neutralizing counterions from Monte Carlo simulations. The surface separation is 15 Å; circles, monovalent; squares, divalent; diamonds, trivalent counterions.

TWO SIMPLE MODELS FOR ION–ION CORRELATIONS

In order to give a conceptual illustration of ion−ion correlation effects, we suggest a simplification of the usual planar double layer invoking just one counterion. Consider two parallel circular surfaces, with radius R, symmetrically arranged as in Figure 4. The two surfaces are uniformly charged, and the only counterion of charge ze present is constrained to the symmetry axis. The whole system is electroneutral, which means that

$$2\pi R^2\sigma = ze. \tag{12}$$

The two surfaces are separated a distance, $2h$, thus the ion−surface interaction, V_{iw}, is

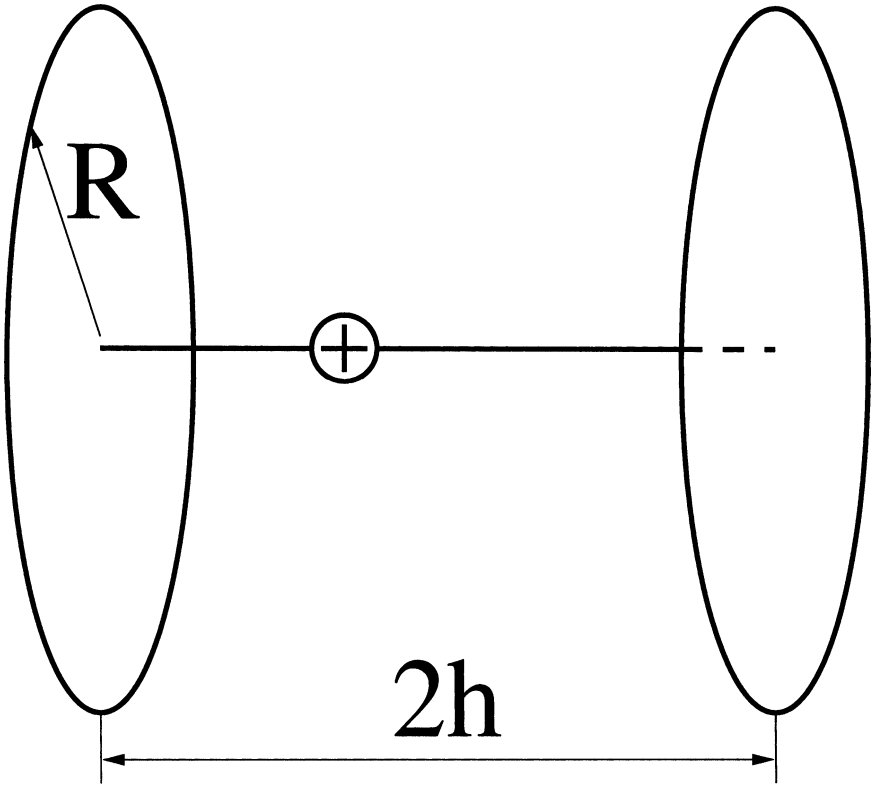

FIGURE 4 Schematic picture of an ultimately simplified electric double layer consisting of two circular parallel sheets carrying a negative charge of *ze* uniformly spread out over the two circles. The neutralizing counterion of charge *ze* is allowed to move on the symmetry line between the circular plates.

$$\frac{V_{iw}}{k_B T} = -\frac{ze\sigma}{4\pi\epsilon_0\epsilon_r k_B T}\left[\int_0^R \frac{2\pi r dr}{\sqrt{r^2+(x-h)^2}} + \int_0^R \frac{2\pi r dr}{\sqrt{r^2+(x+h)^2}}\right]. \quad (13)$$

Let us introduce the two dimensional variables,

$$\gamma_1 = \frac{h}{\lambda_{GC}} \text{ and } \gamma_2 = z\sqrt{\frac{l_B}{\lambda_{GC}}}, \quad (14)$$

and also scale the coordinates, $\hat{x} = x/h$. γ_1 and γ_2 are, of course, related to K_1 and K_2 of Equation (11).

The configurational integral the takes a very simple form,

$$Z = h \exp(-\frac{V_{ww}}{k_B T}) \int_{-1}^{1} d\hat{x} \exp\left[\left(\sqrt{\gamma_2^2 + \gamma_1^2(\hat{x}-1)^2}\right.\right.$$
$$\left.\left. + \sqrt{\gamma_2^2 + \gamma_1^2(\hat{x}+1)^2} - 2\gamma_1\right)\right], \quad (15)$$

where V_{ww} is the surface–surface interaction, which also can be expressed in terms of γ_1 and γ_2. The integral can easily be computed numerically and with all quantities of interest. As an example we show the counterion distribution in Figure 5a for different counterion valency. The qualitative behavior is as could be expected for an electric

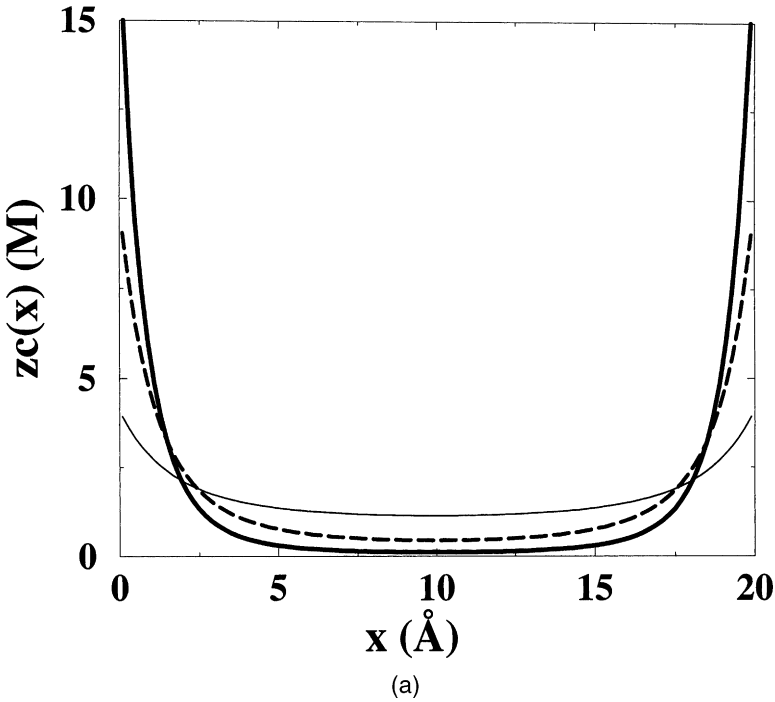

FIGURE 5 (a) The counterion distribution between the two circular wall (see Figure 4). The Bjerrum length is 7.14 Å, the surface charge density is 0.01 e/Å^2, and the counterion valency has been varied. Thin solid line, monovalent; dashed line, divalent; thick solid line, trivalent. (b) The pressure between the two wall with parameters and symbols as in (a). The filled circles represent MC results for two infinite walls with trivalent counterions and with the same l_B and σ as the simple model. (*Continued).*

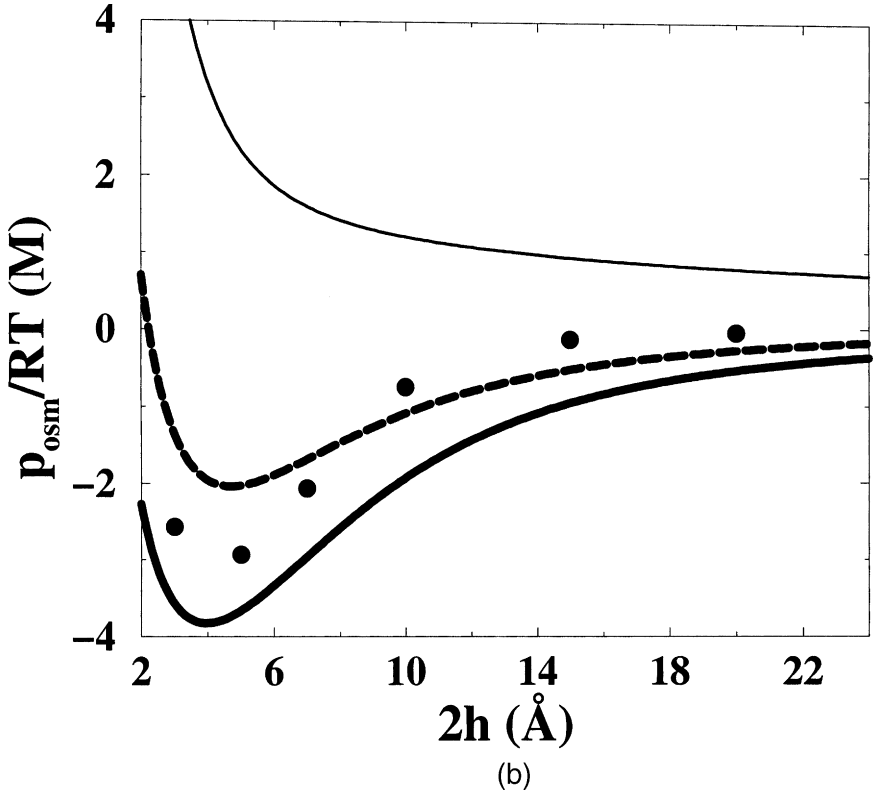

FIGURE 5 (Continued).

double layer with an accumulation of counterion density close to the oppositely charged surfaces.

The force as a function of separation is repulsive and motonically decaying for weakly coupled systems, but with increasing coupling strength the force becomes nonmonotonic and even attractive as we by now should expect from a strongly correlated system. The coupling strength can be increased by multivalent ion as in Figure 5b. Increasing the surface charge density is another possibility, as demonstrated in Figure 6a. A third alternative, still easily accessible experimentally, is to change the solvent to a less polar one (Figure 6b). The model is, of course, not quantitatively correct, but it illustrates how the force turns from being monotonically repulsive to showing an attractive regime when the coupling strength increases and the change occurs for approximately the expected parameter values.

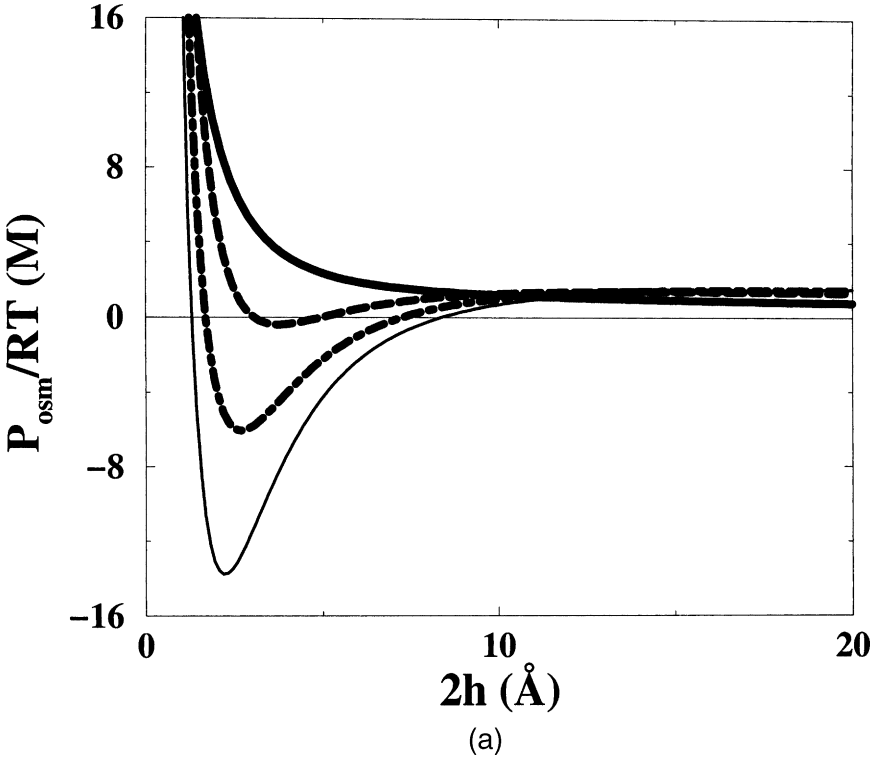

FIGURE 6 The pressure between the two walls for the simple model system as a function of separation. (a) The curves represent different surface charge densities; 0.01 e/Å^2, solid line; 0.025 e/Å^2, dashed line; 0.033 e/Å^2, dot-dashed line; 0.04 e/Å^2, thin line. (b) As in (a) with $\sigma = 0.01$ e/Å^2, but with a variation of the dielectric permittivity; $\varepsilon_r = 80$, 60, 40, and 30 are denoted by thick solid, dashed, dot-dashed, and thin solid lines, respectively. (*Continued).*

The model can be simplified one step further by replacing the two circular surfaces by point charges appropriately placed. Thus, if the counterion is allowed to move along the x-axis between $\pm h$, then the two "surface" charges should be placed at $\pm(h + d)$. The distance d is conveniently chosen so that the electrostatic potential created by the nearest surface in position $\pm h$ is unchanged. This condition gives the following relation for d,

$$d = \sqrt{\frac{ze}{8\pi\sigma}}. \tag{16}$$

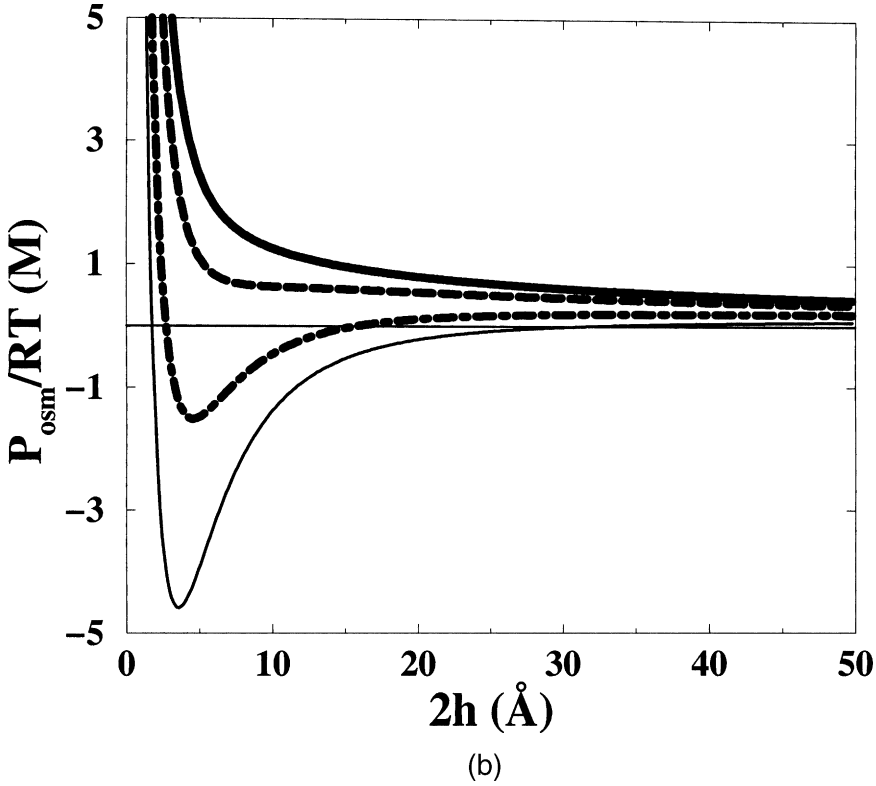

FIGURE 6 (Continued).

The ion–surface and surface–surface interactions are easily obtained:

$$\frac{V_{iw}+V_{ww}}{k_BT}=\frac{z^2l_B}{2}\left[-\frac{1}{(d+h)+x}-\frac{1}{(d+h)-x}+\frac{1}{4(d+h)}\right]. \qquad (17)$$

The final expression for the configurational integral can be given a very simple appearance by introducing the dimensionless variable,

$$\gamma_3=\frac{z^2l_B}{2(d+h)}, \qquad (18)$$

complemented with the scaled coordinate $\hat{x}=x/(d+h)$ and $\hat{h}=h/(d+h)$:

$$Z=(d+h)\int_{-\hat{h}}^{\hat{h}}d\hat{x}\exp\left[\gamma_3\frac{7+\hat{x}^2}{4(1-\hat{x}^2)}\right]. \qquad (19)$$

This simple model with two fixed charges and one mobile charge on a line has the same qualitative properties as the original double layer system with two infinite, uniformly charged walls. Figure 7 shows how a monovalent ion gives a monotonic pressure, while with divalent and trivalent ions an attraction appears at short separation. The attraction, which at first might seem counterintuitive is a simple consequence of the balance between energy and entropy in the system. For weak interactions, γ_3 small, the ion distribution is nearly uniform, the free energy is entropy dominated, and the net pressure is repulsive. As γ_3 increases, asymmetric configurations start to dominate, and the combination of one of the wall charges, $z = -1$, with the counterion, $z = 2$, gives a net charge of $+1e$, which attracts the opposing

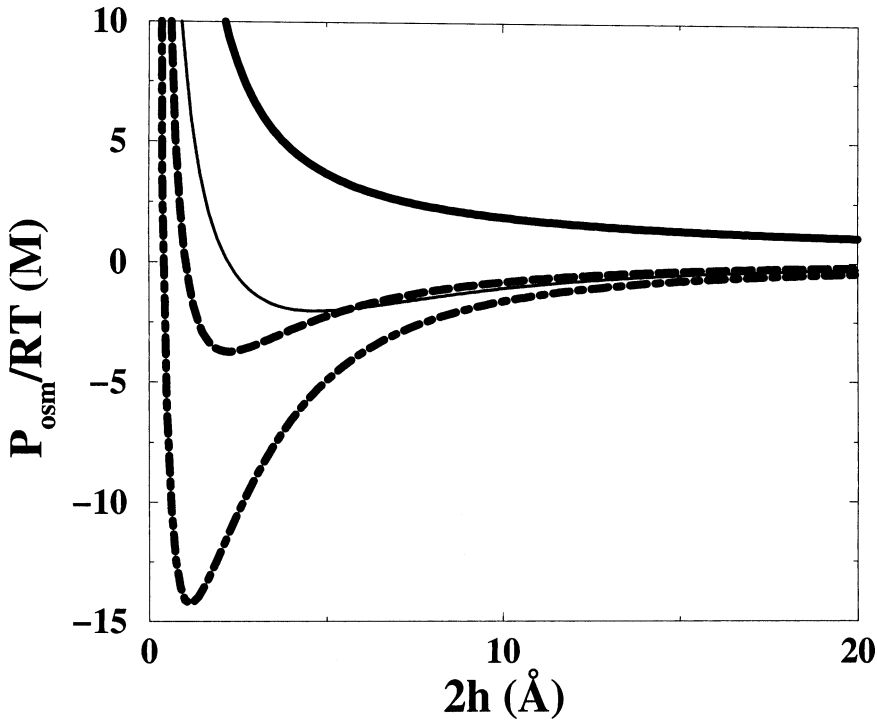

FIGURE 7 The pressure as a function of separation for the simple model system Equation (19). Surface charge density is 0.01 e/Å^2 and $l_B = 7.14$ Å. Monovalent counterion, thick solid line; divalent counterion, dashed line; trivalent counterion, dot-dashed line. The thin solid line is the pressure obtained with the simple model, Equation (15), with a divalent counterion.

negative wall charge. For sufficiently large γ_3 this attraction outweighs the entropic term. Note also that as the asymmetric configurations gain in weight the density at the midplane decreases. Thus, the net attraction found in strongly coupled systems is the combined result of a direct attractive interaction and a decrease in the repulsive entropic term. This behavior, although often overlooked, is also characteristic for correlation effects in more realistic model systems.

Another manifestation of this competition between energy and entropy is a phenomenon referred to as "charge reversal" [35, 36]. This means that the accumulation outside a charged surface of oppositely charged species can be so strong that it overcompensates the surface charge. Hence, at a distance the surface will appear to have reversed its charge. Charge reversal is common in highly coupled systems, and the phenomenon is captured by the simple model Equation (19)—see Figure 8. Note that in order for charge reversal to occur additional salt has to be present in the system. We model this situation with two fixed negative charges at the ends and a divalent cation and a monovalent anion moving on the line in between. The radius of the mobile ions has been set to 2 Å.

EFFECTS OF AGGREGATE GEOMETRY

Ion–ion correlations have such a physical origin that the effect should be independent of the particular geometry of the charged aggregates. Clearly there are quantitative differences when one considers cylindrical, spherical, or irregularly shaped or flexible charged colloidal species, but the basic mechanism should operate in the same way. That this is the case can be seen from Figure 9, where the potential of mean force for two charged spherical aggregates has been calculated from a MC simulation. For monovalent counterions there is a monotonic repulsion, but with multivalent counterions or a solvent with a low dielectric permittivity, the usual entropic double layer repulsion decreases and eventually the correlation term starts to dominate.

The standard way when considering forces between particles of a regular shape is to invoke the Derjaguin approximation [37], which relates the force between curved surfaces to the intercation free energy of planar ones. In this way one can use the results from the planar case also for curved objects, as long as the radius of curvature is larger that both the Debye screening length and the distance of closest approach between the two particles. This clearly demonstrates that the breakdown of the PB equation can occur for any (regular) geometry, and there is reason to expect that such a breakdown can

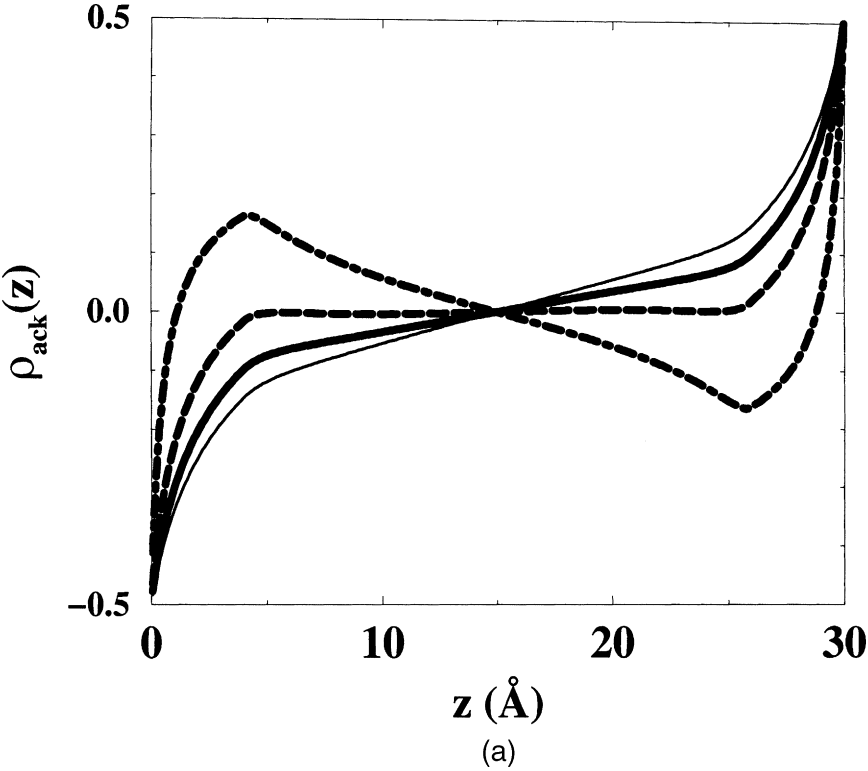

FIGURE 8 Charge reversal in simple model system, Equation (19), with two fixed charges, $-e/2$, at the ends with a divalent counterion plus a monovalent coion moving on a line in between. The abscissa shows the total integrated charge starting from the fixed charge to the left. (a) Variation of the surface charge density, that is, the distance d, and with $l_B = 7.14$ Å. Thin line, 0.01 e/Å^2; thick solid line, 0.013 e/Å^2; dashed line, 0.02 e/Å^2; dot-dashed line, 0.04 e/Å^2. (b) The same as (a), but with a varying dielectric permittivity and $\sigma = 0.01$ e/Å^2. Thin line $\varepsilon_r = 80$, thick solid line $\varepsilon_r = 60$, dashed line $\varepsilon_r = 40$, and dot-dashed line $\varepsilon_r = 20$. (*Continued).*

occur also in the case of irregularly shaped charged particles like, for example, flexible polyelectrolytes.

If two spherical double layers can correlate and give rise to an attractive interaction and similarly two planar ones, then one should also be able to see the same phenomenon for a single polyelectrolyte chain. That is, the chain should, at sufficiently strong coupling, contract [38] and eventually take on an end-to-end distance shorter than the corresponding ideal chain (see Figure 10).

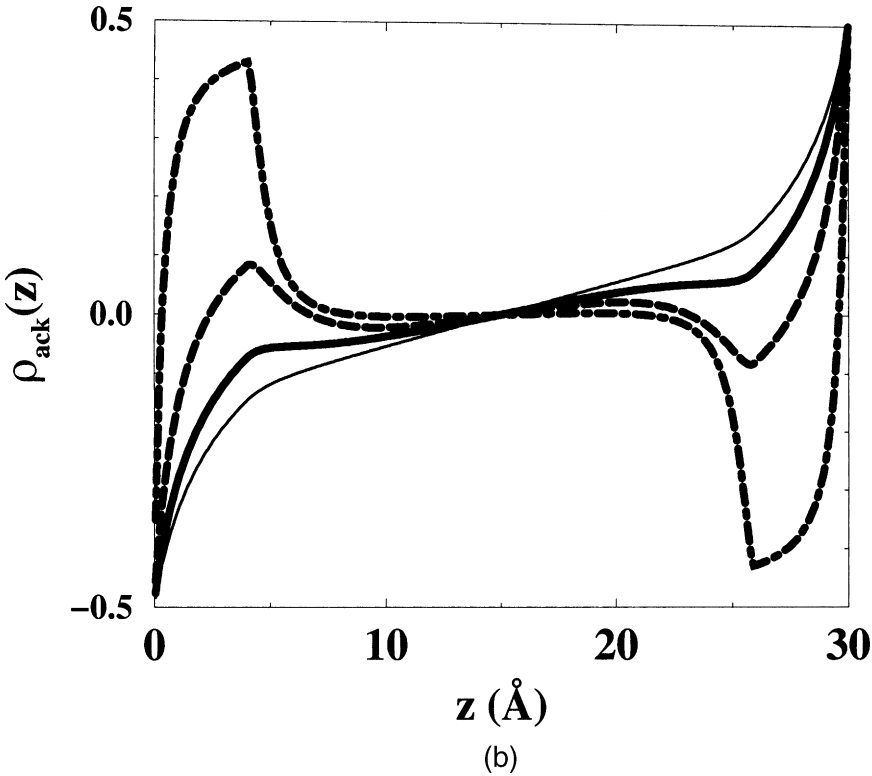

FIGURE 8 (Continued).

EXPERIMENTAL MANIFESTATIONS OF ION–ION CORRELATIONS

An attractive force that can be shown to operate between similarly charged surfaces or particles, which has a range that clearly exceeds the scale for molecular contact between surfaces and is stronger than the conventional van der Waals force, is a good candidate for an ion–ion correlation force. To further substantiate the case, the force should be independent of chemical details such as the molecular nature of the surface and/the chemical nature of the ions. In practice, it can be difficult to eliminate all other possibilities for explaining an observed attractive force. However, the success of the PB/DLVO theory for the description of, at least, aqueous systems has given strong support to the applicability of the primitive model, and we should be able to trust the theoretical results not only with respect

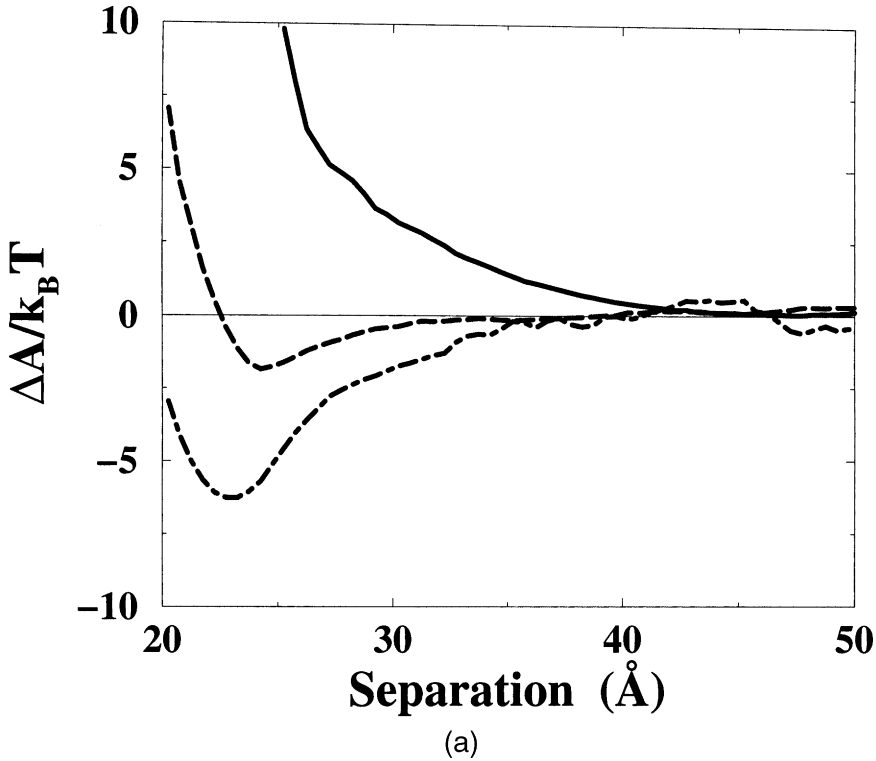

FIGURE 9 (a) The potential of mean force between two spherical aggregates of radius 10 Å and net charge 24. The system contains no salt but only counterions of different valency; solid line, monovalent ions; dashed line, divalent ions; dot-dashed line, trivalent ions. The dielectric permittivity is 78 and the temperature 298 K. (b) The same as in (a), but ε_r is varied; solid line, 78; dashed line, 48; dot-dashed line, 18. (*Continued).*

to the mechanism of the ion−ion correlation force but also with respect to the quantitative predictions. Consequently, we argue that when an attractive force is observed under conditions where the theory predicts as attraction, this is a strong indication that one has a manifestation of the effect.

One of the first clear experimental demonstrations of the correlation effect was due to Khan *et al.* [39], who studied the swelling of the lamellar a liquid crystalline phase formed by the doubled-tailed anionic surfactant AOT [bis (2-ethylhexyl) sulfosuccinate]. With the normal counterion NA^+, the lameller phase swells to *ca* 80% water. This could be quantitatively modeled using the PB approximation

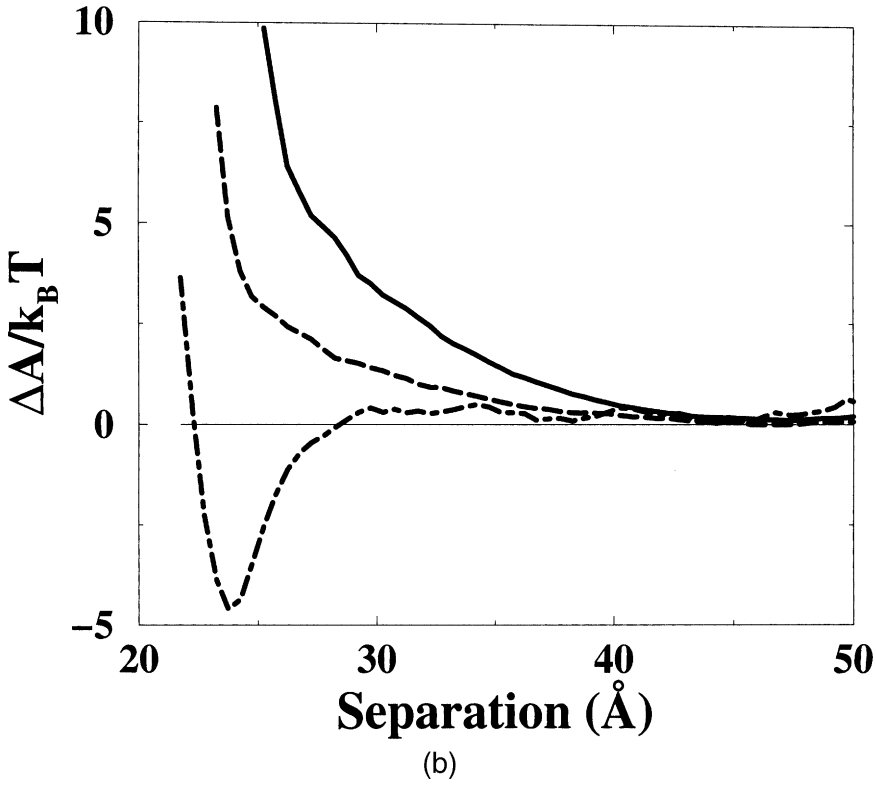

FIGURE 9 (Continued).

[40], while with divalent counterions such as Ca^{2+} and Mg^{2+} a lamellar liquid crystalline phase was still formed, but it only incorporated around 40% water [39, 41]. The prediction of the PB theory was that these systems should swell even more than for the monovalent counterions. To quantitatively study the transition in swelling behavior Khan *et al.* [39] prepared the ternary system NaAOT-CaAOT-water and observed that at intermediate mixing ratios there was a transition from strong to weak swelling and simultaneously a coexistence of two lamellar phases. In fact, in the simulations by Guldbrand *et al.* [19] the parameters where chosen to represent the AOT system. The simulations predicted that for monovalent ions there is a small correction to the PB approximation, while for divalent ions attraction dominates. Furthermore, in the transition from attraction to repulsion the force curve shows nonmonotonic behavior on the repulsive side. This means that two lamellar phases are coexisting with a force that is net

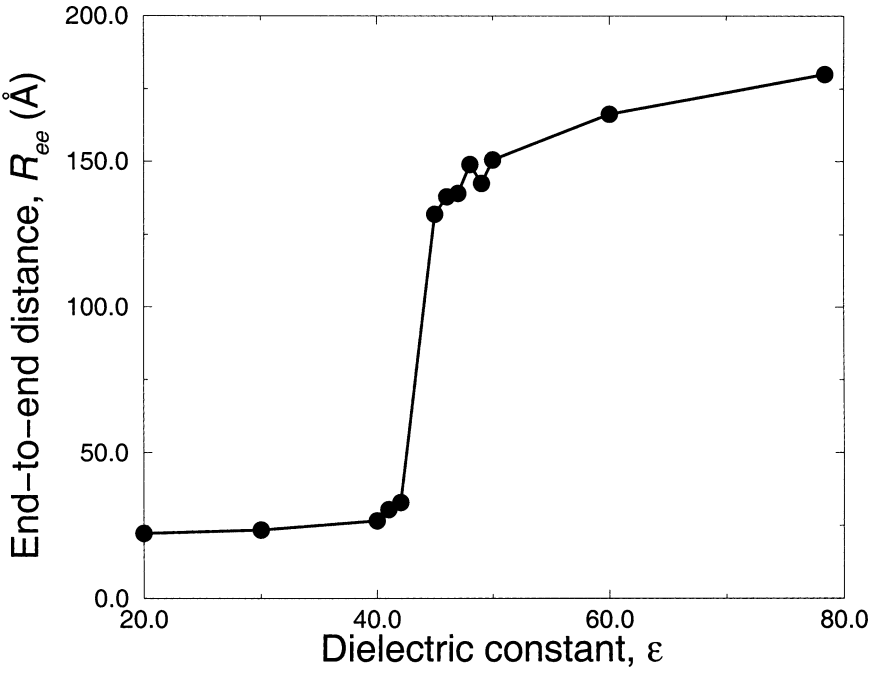

FIGURE 10 The end-to-end distance of 60 monomer polyelectrolyte as a function of the dielectric constant. Here the monomer charge is fixed to −1 and simple monovalent counterions are used. All particles have a hard core radius of 4 Å and the bond length is 6 Å and an additional square well between monomers and counterions has been introduced—see also Khan *et al.* [61].

repulsive at all separations. It is often stated that one needs an attractive region in the force to cause phase separation, but a non-monotonic repulsive force is in fact sufficient.

Using the surface forces apparatus (SFA) technique one has in several studies found a strong attractive force component at close range [42–44]. It manifests itself as an instability occurring for longer separations than expected for the conventional van der Waals force. Although the presence of this attractive component does not change the experimental outcome qualitatively, it is still repulsive at long range, and it requires assumptions about the repulsive double layer force to make quantitative statements about the attractive part. Still, the general observation is that when one expects a sizeable extra attractive force it is also observed. Pashley [45] has studied the double layer force between mica surfaces in the presence of trivalent counterions and reported a *charge inversion* of the mica surfaces, as also

demonstrated for the simple model systems above, which is yet another manifestation of ion–ion correlations [36, 46, 47].

For aqueous systems with monovalent ions one expects correlation effects to give only a quantitative correction to the mean field predictions. There are situations, however, where these corrections can be of importance. Soap films formed by ionic surfactants can have a very high charge density, $\sigma \simeq 0.2-0.3\,\mathrm{C/m^2}$. Earlier we suggested [19] that the formation of Newton black films, with their thin aqueous layer, is triggered by ion–ion correlations. A more recent example is found in concentrated emulsions stabilized by an ionic surfactant. Here one has a similar molecular arrangement of a thin aqueous layer separating two charged surfactant films. Sonneville *et al.* [34] observed a discontinuous swelling in such systems and interpreted the attractive component causing this discontinuity as being due to ion–ion correlations.

As mentioned above, the first explicit discussion of attractive ion–ion correlation forces was inspired by experiments in polyelectrolyte systems [16]. In this case the basic models assume a cylindrical geometry. As discussed above there are for these types of systems numerous examples where the addition of divalent and trivalent counterions induce precipitation [48, 49], but it is difficult to separate the role of short-range interactions from the typical ion–ion correlation effects operating at a slightly longer range. So far the most-studied cases are DNA and virus systems [20, 50, 51], and it has been shown experimentally for a number of cases that multivalent counterions can cause condensation of DNA molecules [52–56]. Recently, the coil–globule transition of a single DNA molecule has been followed in a flourescence microscopy study [57–60]. The transition has been caused by both multivalent counterions and lowering of the solvent dielectric permittivity (see Figure 10).

Salt effects on ion–ion correlation can be quite spectacular. In a system with multivalent counterions and low salt content attractive forces will dominate. Upon addition of a 1:1 salt, there will be a competition between the original multivalent counterions and the monovalent ones coming from the salt. At sufficiently high salt concentration the attraction can disappear and the system will revert to a "normal" double layer repulsion. Thus, we have the unexpected situation that addition of salt leads to *increased* repulsion. The phenomenon can be observed in dilute DNA solutions, where initially compacted DNA (by spermidine or spermine) expands if the salt concentration becomes sufficiently hihg [61].

For spherical particles it has turned out to be more difficult to find clear demonstrations of ion–ion correlations [62]. It is well established for many colloidal systems that di- and trivalent ions can cause

precipitation, coagulation, or both [63]. Such observations have usually been interpreted in terms of "salt bridges." One common example is the precipitation of soaps by calcium or magnesium ions. For a given charge density, the electrostatic interactions are weaker between spheres than between planes, for example, as can be seen from the Derjaguin approximation. Consequently, one needs a higher charge density in the spherical system relative to the planar or cylindrical cases in order to see a net attraction.

The setting of cement paste is one interesting example of attractive correlation forces between approximately spherical particles. It is generally agreed that the cohesion of cement paste occurs through the formation of a network of nanoparticles of a calcium silicate hydrate. These particles carry a very high surface charge at *pH* conditions typical for cement paste, $pH \approx 10-13$. Divalent calcium ions acts as counterions. Thus, the conditions are such that the net interaction between the particles is expected to be attractive [64]. Atomic force microscope measurements of the interaction between the calcium silicate hydrate particles confirm the expectations. Electrokinetic experiments also show that the mobility of the nanoparticles changes sign as *pH* rises and the surface charge density increases [65]. That is, a charge reversal takes place as predicted by the calculations presented above.

CONCLUSIONS

We have pointed out the generality of ion–ion correlations and tried to demonstrate the physical mechanism in simple model systems. The generality means that geometry, ion type, details of surface charges, etc., are of secondary importance. The forces in charged macromolecular systems are always a balance between repulsive forces of entropic origin and attractive forces of energetic origin. For many systems of chemical interest the repulsive forces dominate and the mean field description provided by the PB equation is adequate. There are many ways of changing the balance between entropic and energetic terms; the most efficient way to favor attractive interactions is to reduce the importance of the entropy term simply by decreasing the number of charged particles by using multivalent counterions. The other way to favor attractive forces is by increasing the importance of the energetic term by, *e.g.*, going to a solvent with a low dielectric permittivity.

Numerically, the important means for investigating ion–ion correlations have been MC simulations and accurate integral equation techniques. One would hope that more simple approaches based on different perturbational schemes should suffice to capture the phenomenon at

least semiquantitatively. This does not seem to be the case, and our general conclusion is that whenever ion–ion correlations become important and cause attractive forces to dominate, we are unfortunately well outside the regime where more simple and analytically tractable approaches are applicable. At the present stage we believe that in order to get further insight into ion–ion correlations, well-designed experiments for, in particular, spherical systems are needed.

REFERENCES

[1] Derjaguin, B. V. and Landau, L., *Acta Phys. Chim. URSS* **14**, 633–662 (1941).
[2] Verwey, E. J. W. and Overbeek, J. T. G., *Theory of the Stability of Lyophobic Colloids* (Elsevier Publishing Company Inc., Amsterdam, 1948).
[3] Israelahvili, J., *Intermolecular and Surface Forces*, 2nd ed. (Academic Press, London, 1991).
[4] Wennerström, H., Daiclc, J., and Ninham, B. W., *Phys. Rev. A* **60**, 1–4 (1999).
[5] Woodward, C. E., Jönsson, B., and Ákesson, T., *J. Chem. Phys.* **89**, 5145–5152 (1988).
[6] Bratko, D., Woodward, C. E., and Luzar, A., *J. Chem. Phys.* **95**, 5318–5326 (1991).
[7] Ninham, B. and Parsegian, V. A., *J Theoret. Biol.* **31**, 405–428 (1971).
[8] Attard, P., Kjellander, R., and Mitchell, D. J., *Chem. Phys. Lett.* **139**, 219–224 (1987).
[9] Attard, P., Kjellander, R., Mitchell, D. J., and Jönsson, B., *J. Chem. Phys.* **89**, 1664–1680 (1988).
[10] Podgornik, R., *Chem. Phys. Lett.* **156**, 71–75 (1988).
[11] Podgornik, R., *Chem. Phys. Lett.* **144**, 503–508 (1989).
[12] Tsao, Y.-H., Evans, D. F., and Wennerström, H., *Science* **262**, 547–550 (1993).
[13] Belloni, L. and Spalla, O., *J. Chem. Phys.* **107**, 465–480 (1997).
[14] Forsman, J., Jönsson, B., and Ákesson, T., *J. Phys. Chem. B* **102**, 5082–5087 (1998).
[15] Onsager, L., *Ann. N. Y. Acad. Sci.* **51**, 627–659 (1949).
[16] Oosawa, F., *Biopolymers* **6**, 1633–1647 (1968).
[17] Mahanty, J. and Ninham, B. W., *Dispersion Forces* (Academic Press, London, 1976).
[18] Grønbech-Jensen, N., Mashl, R. J., Bruinsma, R. F., and Gelbart, W., *Phys. Rev. Lett.* **78**, 2477–2480 (1997).
[19] Guldbrand, L., Jönsson, B., Wennerström, H., and Linse, P., *J. Chem. Phys.* **80**, 2221–2228 (1984).
[20] Guldbrand, L., Nilsson, L., and Nordenskiöld, L., *J. Chem. Phys.* **85**, 6686–6698 (1986).
[21] Jönsson, B., Wennerström, H., and Halle, B., *J. Phys. Chem.* **84**, 2179–2185 (1980).
[22] Wennerström, H., Jönsson, B., and Linse, P., *J. Chem. Phys.* **76**, 4665–4670 (1982).
[23] Kjellander, R. and Marčelja, S., *J. Phys.* (*France*) **49**, 1009–1015 (1988).
[24] Engström, S. and Wennerström, H., *J. Phys. Chem.* **82**, 2711–2714 (1978).
[25] Tiddy, G. J. T., *Phys. Rep.* **57**, 1–46 (1980).
[26] Pellenq, R., Caillot, J., and Delville, A., *J. Phys. Chem. B* **101**, 8584–8594 (1997).
[27] Kjellander, R. and Marčelja, S., *Chem. Phys. Lett.* **112**, 49–43 (1984).
[28] Kjellander, R. and Marčelja, S., *J. Chem. Phys.* **82**, 2122–2135 (1985).
[29] Valleau, J. P., Ivkov, R., and Torrie, G. M., *J. Chem. Phys.* **95**, 520–532 (1991).

[30] Bratko, D. and Vlachy, V., *Chem. Phys. Lett.* **90**, 434–438 (1982).
[31] Outhwaite, C. W. and Bhuiyan, L. B., *J. Chem. Soc., Faraday Trans.* 2 **79**, 707–718 (1983).
[32] Outhwaite, C. W. and Bhuiyan, L. B., *Molec. Phys.* **74**, 367–381 (1991).
[33] Das, T., Bratko, D., Bhuiyan, L. B., and Outhwaite, C. W., *J. Phys. Chem.* **99**, 410–418 (1995).
[34] Sonneville, O., Gulik-Krzywicki, V. B. T., Jönsson, B., Wennerström, H., Lindner, P., and Cabane, B., *Langmuir* **16**, 1566–1579 (2000).
[35] Pashley, R. M. and Israelachvili, J. N., *J. Coll. Interface Sci.* **101**, 511–523 (1984).
[36] Sjöström, L., Åkesson, T., and Jönsson, B., *Ber. Bunsenges. Phys. Chem.* **100**, 889–893 (1996).
[37] Derjaguin, B., *Kolloid-Z* **69**, 155–164 (1934).
[38] Stevens, M. J. and Kremer, K., *J. Chem. Phys.* **103**, 1669–1690 (1995).
[39] Khan, A., Fontell, K., and Lindman, B., *J. Colloid Interface Sci.* **101**, 193–200 (1984).
[40] Khan, A., Jönsson, B., and Wennerström, H., *J. Phys. Chem.* **89**, 5180–5184 (1985).
[41] Khan, A., Fontell, K., and Lindman, B., *Coll. Surf.* **11**, 401–408 (1984).
[42] Marra, J., *Biophys. J.* **50**, 815–825 (1986).
[43] Kjellander, R., Marčelja, S., Pashley, R. M., and Quirk, J. P., *J. Chem. Phys.* **92**, 4399–4407 (1990).
[44] Petrov, P., Miklavic, S. J., and Nylander, T., *J. Phys. Chem.* **98**, 2602–2607 (1994).
[45] Pashley, R. M., *J. Coll. Interface Sci.* **102**, 23–35 (1984).
[46] Tang, Z., Scriven, L. E., and Davis, H. T., *J. Chem. Phys.* **97**, 9258–9266 (1992).
[47] Shklovskii, B. I., *Phys. Rev. E* **60**, 5802–5811 (1999).
[48] de la Cruz, M. O., Belloni, L., Delsanti, M., Dalbiez, J. P., Spalla, O., and Drifford, M., *J. Chem. Phys.* **103**, 5781–5791 (1995).
[49] Wittmer, J., Johner, A., and Joanny, J.-F., *J. Phys II* **5**, 635–654 (1995).
[50] Tang, J. X., Wong, S., Tran, P. T., and Janmey, P. A., *Ber. Bunsen-Ges. Phys. Chem.* **100**, 796–806 (1996).
[51] Lyubartsev, A. P., Tang, J. X., Janmey, P. A., and Nordenskiöld, L., *Phys. Rev. Lett.* **81**, 5465–5468 (1998).
[52] Gosule, L. C. and Schellman, J. A., *Nature* **259**, 333–335 (1976).
[53] Wilson, R. W. and Bloomfield, V. A., *Biochemistry* **18**, 2192–2196 (1979).
[54] Bloomfield, V. A., Wilson, R. W., and Rau, D. C., *Biophys. Chem.* **11**, 339–343 (1980).
[55] Widom, J. and Baldwin, R. L., *J. Mol. Biol.* **144**, 431–453 (1980).
[56] Sen, D. and Cothers, D. M., *Biochemistry* **25**, 1495–1503 (1986).
[57] Mel'nikov, S. M., Sergeyev, V. G., and Yoshikawa, K., *J. Am. Chem. Soc.* **117**, 2401–2408 (1995).
[58] Yoshikawa, K., Takahashi, M., Vasilvskaya, V. V., and Khokhlov, A. R., *Phys. Rev. Lett.* **76**, 3029–3031 (1996).
[59] Kidoaki, S. and Yoshikawa, K., *Biophys. J.* **76**, 932–939 (1996).
[60] Mel'nikov, S. M., Khan, M. O., Lindman, B., and Jönsson, B., *J. Am. Chem. Soc.* **121**, 1130–1136 (1999).
[61] Khan, M. O., Mel'nikov, S. M., and Jönsson, B., *Macromolecules* **32**, 8836–8840 (1999).
[62] Chan, D. Y. C., *Phys. Rev. E* **63**, 1806–1813 (2001).
[63] Shaw, D. J., *Introduction to Colloid and Surface Chemistry*, 4th ed. (Butterworths, London, 1992).
[64] Jönsson, B., Wennerström, H., Nonat, A., and Cabane, B., *Langmuir* **xx**, submitted (2004).
[65] Nachbaur, L., Nkinamubanzi, P.-C., Nonat, A., and Mutin, J.-C., *J. Coll. Interf. Sci.* **202**, 261–268 (1998).